Asymmetric Magnetization Reversal in Exchange-Biased Hysteresis Loops

M. R. Fitzsimmons and P. Yashar
Los Alamos National Laboratory, Los Alamos, New Mexico 87545

C. Leighton and Ivan K. Schuller
Department of Physics, University of California–San Diego, La Jolla, California 92093-0319

J. Nogués
Departament de Física, Universitat Autònoma de Barcelona, 08193 Bellaterra, Spain

C. F. Majkrzak and J. A. Dura
National Institute of Standards and Technology, Gaithersburg, Maryland 20899
(Received 25 October 1999)

Polarized neutron reflectometry is used to probe the in-plane projection of the net-magnetization vector $\vec{M}$ of polycrystalline Fe films exchange coupled to twinned (110) MnF_2 or FeF_2 antiferromagnetic (AF) layers. The magnetization reversal mechanism depends upon the orientation of the cooling field with respect to the twinned microstructure of the AF, and whether the applied field is increased to (or decreased from) a positive saturating field; i.e., the magnetization reversal is asymmetric. The reversal of the sample magnetization from one saturated state to the other occurs via either domain wall motion or magnetization rotation on opposite sides of the same hysteresis loop.

PACS numbers: 75.70.Ak, 61.12.–q

Exchange bias [1,2] refers to a shift of the ferromagnetic hysteresis loop along the field axis by an amount H_e. The exchange bias is a consequence of an interaction across the interface between dissimilarly ordered magnetic materials, e.g., a ferromagnet (F) and an antiferromagnet (AF) [1,2]. This exchange interaction induces a unidirectional anisotropy as the AF material is cooled through its Néel temperature, T_N [1,2]. Exchange-biased bilayers exhibit a number of unusual properties, such as positive exchange bias [3,4], perpendicular coupling [5,6], rotational hysteresis at high fields [7], magnetic training effects [8], measurement dependent loop shifts [9,10], memory effects [11], and asymmetrically shaped hysteresis loops [12–15].

With conventional magnetometry, the projection of the net sample magnetization vector, $\vec{M}$, onto the direction of the applied field is measured; i.e., the measured quantity is $\vec{M} \cdot \vec{H}_a / H_a$. The condition $\vec{M} \cdot \vec{H}_a = 0$ can be obtained when the magnetic film breaks up into differently aligned domains with net magnetization equal to zero. Alternatively, the net sample magnetization can remain unchanged in magnitude, but rotate away from the applied field, so $\vec{M} \cdot \vec{H}_a = 0$. Domain observations in some AF/F systems seem to indicate that the locations of domain nucleation in the increasing or decreasing branches of the loop are different [16]. This is consistent with the frequent observation of asymmetrically shaped hysteresis loops as seen by many experimenters [12–15]. In this paper, we use polarized neutron reflectometry to investigate this phenomenon beyond the scope of conventional magnetometry.

We report on neutron scattering measurements of $\vec{M}$ for two kinds of exchange coupled bilayer systems, i.e., Fe deposited onto antiferromagnets with very different anisotropy fields, H_k, FeF_2 ($H_k = 149$ kOe) and MnF_2 ($H_k = 7$ kOe) [17]. We find the reversal of the sample magnetization from one saturated state to the other can occur via both mechanisms, i.e., the nucleation and propagation of domain walls or the rotation of the net sample magnetization away from the applied field. In fact, we observe both mechanisms on opposite sides of the same hysteresis loop. The particular mechanism observed depends upon the orientation of the cooling field with respect to the crystallographic directions of the AF twins, and whether the measurement is made on the increasing or decreasing branch of the loop [18].

Three bilayer samples (one with MnF_2 and two with FeF_2) were prepared by sequential electron beam evaporation of Fe (~0.1 nm/s) onto the AF (~0.2 nm/s) [4,19]. The AF's were deposited on 20 mm × 20 mm polished single crystal (100) MgO substrates. In the case of the Fe-MnF_2 sample, a buffer layer of ZnF_2 (25 nm) was first deposited onto the MgO in order to improve the epitaxy of MnF_2 [4]. The nominal thicknesses were MnF_2 (50 nm), FeF_2 (90 nm), Fe (11 nm), and Al or Ag (3 nm). The base pressure of the deposition chamber was 4×10^{-6} Pa, while the pressure during deposition of the fluorides was approximately 8×10^{-5} Pa. The deposition temperatures were ZnF_2 (473 ± 2 K), MnF_2 (573 ± 2 K), FeF_2 (473 ± 2 K), Fe (423 ± 2 K), and Al or Ag (423 ± 2 K). The Al or Ag acts as a capping layer to prevent oxidation of the Fe. Using x-ray reflectometry [20], the thicknesses of the Fe films were determined to range from 9.5 nm to 12 nm for the different samples, and the roughness of the F-AF interface (root-mean-square deviation about its mean) to be 1.9 ± 0.2 nm and

 0031-9007/00/84(17)/3986(4)$15.00 © 2000 The American Physical Society

1.0 ± 0.2 nm for the Fe-MnF_2 and Fe-FeF_2 interfaces, respectively. In-plane glancing x-ray diffraction [21] and reflection high-energy electron diffraction confirmed that the AF layers grow as twinned quasiepitaxial thin films. One AF crystal domain is oriented such that $[1\bar{1}0]$ MnF_2 (or FeF_2) $\parallel$ [110] MgO, while the other domain is oriented with [001] MnF_2 (or FeF_2) $\parallel$ [110] MgO.

To confirm that the Fe overlayer is exchange coupled to the AF after field cooling through the Néel point of MnF_2 ($T_N = 67$ K) or FeF_2 ($T_N = 78$ K), the ferromagnetic hysteresis loops of the samples were measured with a SQUID magnetometer. The hysteresis loop for the Fe-MnF_2 sample cooled in a field of $H_{FC} = 6.40 \pm 0.01$ kOe ($= 509$ kA/m) is shown in Fig. 1(a). The exchange bias and coercivity (H_c) were determined to be $H_e = -30 \pm 1$ Oe and $H_c = 148 \pm 1$ Oe. H_e and H_c are consistent with previous measurements on similarly grown bilayers [4,19].

For the neutron scattering experiment, two cooling field orientations were used. The first orientation involved applying a cooling field $H_{FC} = 6.40 \pm 0.05$ kOe along a direction bisecting the anisotropy (easy) axes (the [001] axes) of the two AF domains [see Fig. 1(a), inset] as the sample was cooled from room temperature to 10 ± 1 K. The second orientation involved applying the same cooling field along a direction parallel to the anisotropy axis of one AF domain, and thus perpendicular to the easy axis of the other domain [see Fig. 2(a), inset].

The magnitude and orientation of the net sample magnetization relative to the cooling field were determined from measurements of the sample reflectivities with polarized neutrons. Polarized neutron reflectometry involves specular reflection of a polarized neutron beam from a flat sample onto a polarization analyzer [22,23]. Four neutron cross sections were measured. Two cross sections correspond to the non-spin-flip (NSF) reflectivity profiles, where the intensities of the reflected radiation for spin-up $(++)$ [and alternatively spin-down $(--)$] neutrons illuminating and reflecting from the sample were measured. The difference between the NSF reflectivity profiles, ΔNSF, is related to the projection on to the direction of the applied field of the net (ferromagnetic) sample magnetization averaged over the lateral dimensions of the sample, i.e., $\Delta\mathrm{NSF} \propto \vec{M} \cdot \vec{H}_a/H_a = M_{\parallel}$.

The remaining two cross sections are the spin-flip (SF) reflectivities, which are nonzero if the sample changes the neutron beam polarization from spin-up to spin-down $(+-)$, and vice versa. For example, the beam polarization will change and SF scattering will be observed, if the magnetic induction vector is perpendicular to the neutron spin, so $\mathrm{SF} \propto (\vec{M} \times \vec{n}) \cdot \vec{H}_a/H_a = M_{\perp}$, where $\vec{n}$ is the normal to the film surface.

Neutron reflectivity profiles for several fields, $\vec{H}_a$, applied parallel and antiparallel to $\vec{H}_{FC}$, were measured. Examples, typical of the profiles observed from the Fe-MnF_2 sample, are shown in Fig. 1(b). The net sample magnetizations deduced from the neutron measurements

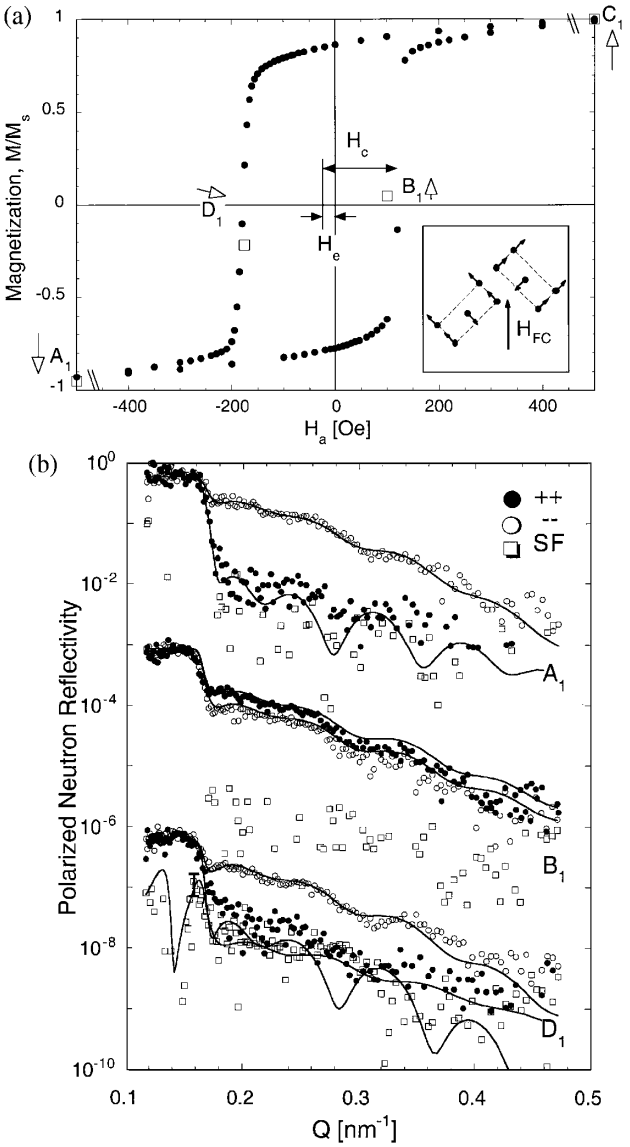

FIG. 1. (a) Hysteresis loop (•) for the Fe-MnF_2 sample and the orientation of the cooling field, $H_{FC} = 6.4$ kOe, relative to the MnF_2 domains (inset). The net magnetization $\vec{M}$ (→) relative to $\vec{H}_{FC}$ deduced from the neutron data corresponding to H_a (□) is superimposed. (b) Polarized neutron reflectivity profiles measured for the same sample and cooling field. A_1: negative saturation $H_a = -6.4$ kOe (note the break in the figure scale); B_1: $H_a = H_e + H_c$, and D_1: $H_a = H_e - H_c$. A representative error bar is shown for the spin-flip scattering. Solid curves are fits of a model to the data.

are shown by the length and direction of the open arrows relative to $\vec{H}_a$ adjacent to the letters A_1–D_1 and symbols "□" in Fig. 1(a).

The large splitting between the NSF profiles requires $\Delta\mathrm{NSF} \gg 0$, for $H_a = -6.4$ kOe [curves A_1 in Fig. 1(b)], and the lack of SF scattering above background [$\sim 10^{-3}$ for the measurements shown in Fig. 1(b)] requires $\mathrm{SF} \sim 0$ and indicates that the sample was saturated for this applied field. For point B_1 in Fig. 1(a), corresponding to $H_a \sim H_c - H_e$, the NSF profiles [curves B_1 in Fig. 1(b)]

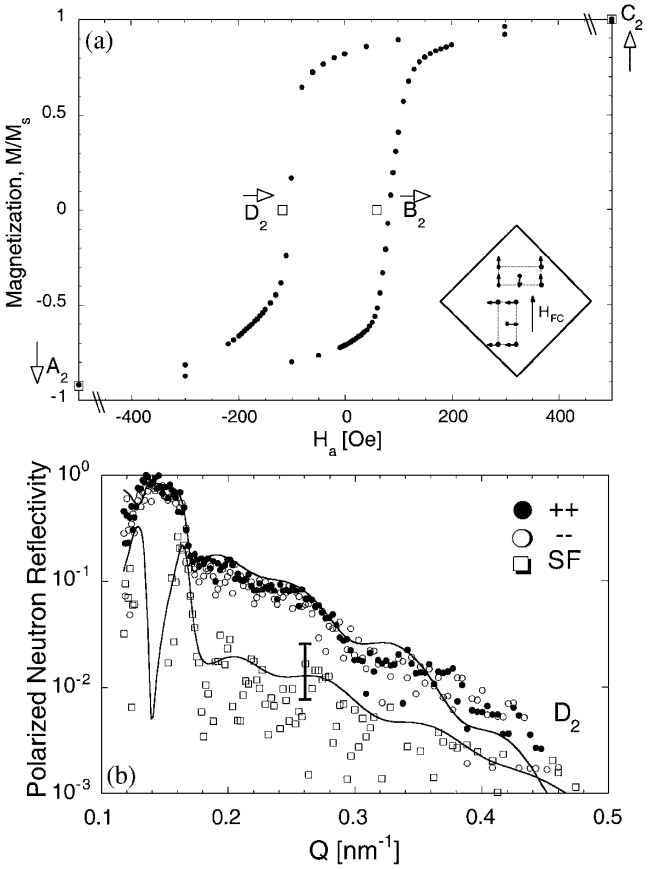

FIG. 2. (a) Hysteresis loop (•) for the Fe-MnF_2 sample and the orientation of the cooling field, $H_{FC} = 6.4$ kOe, relative to the MnF_2 domains (inset). The net magnetization $\vec{M}$ (→) relative to $\vec{H}_{FC}$ deduced from the neutron data corresponding to H_a (□) is superimposed. (b) Polarized neutron reflectivity profiles measured for the same sample and cooling field. D_1: $H_a = H_e - H_c$.

were nearly superimposed, $\Delta\text{NSF} \sim 0$, and no SF scattering above background was observed, $\text{SF} \sim 0$. $\Delta\text{NSF} \sim 0$ indicates the net sample magnetization parallel to the applied field was zero. $\text{SF} \sim 0$ further indicates that the film did not contain domains with components of magnetization perpendicular to the applied field [24]. Together, the conditions $\Delta\text{NSF} \sim 0$ and $\text{SF} \sim 0$ mean that the Fe film is composed of nearly equal populations of domains with magnetization aligned parallel or antiparallel to the applied field [25]. The NSF profiles (not shown) corresponding to C_1 (at $H_a = +6.4$ kOe) in Fig. 1(a) were similar to those shown in Fig. 1(b) corresponding to A_1, thus, indicating saturation of the sample at C_1. Reduction of the applied field from C_1 to D_1 (Fig. 1) resulted in SF scattering nearly an order of magnitude above background, $\text{SF} \gg 0$. In contrast to observations at point B_1 ($H_a = H_e + H_c$), where $\text{SF} \sim 0$, the presence of significant SF scattering at point D_1 ($H_a \sim H_e - H_c$) indicates rotation of the sample magnetization away from the applied field. In other words, we observe *a different magnetization reversal mechanism* on increasing the field to saturation than decreasing the field from saturation. Explicitly, we have domain wall nucleation and propagation at B_1, in contrast to magnetization rotation at D_1 [26]. This asymmetry in reversal mechanisms was also observed in the Fe-FeF_2 system under identical cooling conditions. The results obtained for the first cooling field orientation [see Fig. 1(a), inset] and their implications for the magnitude of $M_\parallel$ and $M_\perp$ are summarized in Table I. Detailed quantitative fitting of model magnetic structures, whose calculated reflectivity profiles are shown in Fig. 1(b) as the solid curves, to the neutron data confirms the qualitative picture described previously.

The reflectivity profiles measured from the sample after field cooling in the second orientation field applied parallel to the easy axis of one MnF_2 domain (and perpendicular to the other [see Fig. 2(a) inset]) are shown in Fig. 2(b). These profiles correspond to point D_2 ($H_a = H_e - H_c$) in Fig. 2(a). As was the case for the first cooling field orientation at a similar field (D_1), significant SF scattering, $\text{SF} \gg 0$, was observed indicating a rotation of the sample magnetization as the field was changed to $H_a = H_e - H_c$. However, in stark contrast to the first cooling field orientation, the profile recorded for point B_2 was no different than that recorded for point D_2. In other words, after the sample is cooled in a field corresponding to the second orientation [see Fig. 2(a), inset], the reversal of the sample magnetization from one saturated state to the other involved rotation of the sample magnetization regardless of whether the applied field was increased or decreased. *The reversal of the sample magnetization is symmetric.* The magnetization reversal field with the cooling field applied in the second configuration for the Fe-FeF_2 sample was qualitatively the same as that observed for the Fe-MnF_2 sample. Note that since the anisotropy fields of MnF_2 and FeF_2 are so different, and the mechanisms through which the Fe film magnetization was reversed were identical for both AFs, we conclude that the anisotropy field plays little role in the magnetization reversal in these systems. The results for the second cooling field orientation are summarized in Table I.

For the first cooling field condition [see Fig. 1(a), inset] and at $H_a \sim H_e + H_c$, the Fe magnetization was at 45° to the anisotropy axes of both AF domains. We propose that this direction constitutes an "easy axis" for the magnetization direction due to the frustration of the perpendicular coupling [5,6,27,28] in a twinned system.

TABLE I. Summary of observations for Fe-MnF_2 and Fe-FeF_2 bilayers for the first (subscript 1) and second (subscript 2) H_{FC} conditions.

Point	$\Delta\text{NSF} = \lvert(++) - (--)\rvert$	$M_\parallel$	$\text{SF} = \langle(+-) + (-+)\rangle$	$M_\perp$
A_1 and C_1	$\gg 0$	$\neq 0$	~ 0	~ 0
B_1	~ 0	~ 0	~ 0	~ 0
D_1	~ 0	~ 0	$\gg 0$	$\neq 0$
A_2 and C_2	$\gg 0$	$\neq 0$	~ 0	~ 0
B_2 and D_2	0	0	$\gg 0$	$\neq 0$

The "45° coupling" is energetically favorable as each AF domain independently tends to perpendicular coupling. (N.B. twin-driven frustration of collinear coupling also results in 45° coupling.) An added factor is that the field cooling provides an additional unidirectional asymmetry. Therefore, for the first cooling condition [Fig. 1(a), inset], field reduction from saturation results in magnetization rotation rather than domain nucleation. This is due to the intrinsic unidirectionality that hinders formation of domains with magnetization antiparallel to the cooling field direction. Gradual rotation is energetically favorable. As the field is reduced from negative saturation, formation of domains with magnetization parallel to the initial cooling direction is favored. Hence reversal occurs by domain nucleation and propagation. On the other hand, in the second cooling field condition [Fig. 2(a), inset] the situation is essentially different in that rotation towards the "45° easy axis" is always favored. The initial reduction of the field from saturation results in rotation towards a direction 45° to both anisotropy axes of the AF domains *on both sides of the loop.*

In conclusion, the magnetization reversal process of an Fe overlayer exchange coupled to MnF_2 or FeF_2 depends upon (1) the cooling field direction relative to the AF anisotropy axis, and (2) whether the applied field was increased from negative to positive values (relative to the direction of the cooling field) or vice versa. A simple model is capable of explaining the observed reversal symmetry when the cooling field is at 45° with respect to both twin anisotropy axes, as well as the symmetric reversal found when the field is parallel to the anisotropy axis of one of the twins. This model is based upon the existence of a unidirectional anisotropy in conjunction with the "45° coupling" intuitively expected in a twinned system. As was observed for exchange coupled Fe-MnF_2 and Fe-FeF_2 films, the presence of complex microstructures, e.g., twins, may be a determining factor in the magnetization reversal process and exchange bias in many other F-AF exchange coupled systems.

The neutron scattering facilities of the Manuel Lujan Jr. Neutron Scattering Center and the National Institute of Standards and Technology are gratefully appreciated. Discussions with Dr. R. D. Shull, Professor M. Kiwi, and Dr. J. Borchers are gratefully acknowledged. The polarizing supermirrors at Los Alamos were kindly provided to us by Dr. P. Boni and Dr. D. Clemens. This work was supported by the U.S. Department of Energy, BES-DMS under Contract No. W-7405-Eng-36, Grant No. DE-FG03-87ER-45332, and funds from the University of California Collaborative University and Laboratory Assisted Research.

[1] W. H. Meiklejohn and C. P. Bean, Phys. Rev. **105**, 904 (1957).
[2] J. Nogués and Ivan K. Schuller, J. Magn. Magn. Mater. **192**, 203 (1998).
[3] J. Nogués, D. Lederman, T. J. Moran, and Ivan K. Schuller, Phys. Rev. Lett. **76**, 4624 (1996).
[4] C. Leighton, J. Nogués, Harry Suhl, and Ivan K. Schuller, Phys. Rev. B **60**, 12 837 (1999).
[5] Y. Ijiri, J. A. Borchers, R. W. Erwin, S. H. Lee, P. J. van der Zaag, and R. M. Wolf, Phys. Rev. Lett. **80**, 608 (1998).
[6] T. J. Moran, J. Nogués, D. Lederman, and Ivan K. Schuller, Appl. Phys. Lett. **72**, 617 (1998).
[7] M. Takahashi, A. Yanai, S. Taguchi, and T. Suzuki, Jpn. J. Appl. Phys. **19**, 1093 (1980).
[8] C. Schlenker and D. Paccard, J. Phys. (Paris) **28**, 611 (1967).
[9] E. D. Dahlberg, B. Miller, B. Hill, B. J. Jönsson, V. Ström, K. V. Rao, J. Nogués, and Ivan K. Schuller, J. Appl. Phys. **85**, 6893 (1998).
[10] P. Miltényi, M. Gruyters, G. Güntherodt, J. Nogués, and Ivan K. Schuller, Phys. Rev. B **59**, 3333 (1999).
[11] N. J. Gökemeijer and C. L. Chien, J. Appl. Phys. **85**, 5516 (1999).
[12] C. Tsang and K. Lee, J. Appl. Phys. **53**, 2605 (1982).
[13] T. Ambrose and C. L. Chien, J. Appl. Phys. **83**, 7223 (1998).
[14] J. Nogués, T. J. Moran, D. Lederman, Ivan K. Schuller, and K. V. Rao, Phys. Rev. B **59**, 6984 (1999).
[15] M. D. Stiles and R. D. McMichael, Phys. Rev. B **59**, 3722 (1999).
[16] V. I. Nikitenko, V. S. Gornakov, L. M. Dedukh, Yu. P. Kabanov, A. F. Khapikov, A. J. Shapiro, R. D. Shull, A. Chaiken, and R. P. Michel, Phys. Rev. B **57**, R8111 (1998).
[17] A. S. Carriço, R. E. Camley, and R. L. Stamps, Phys. Rev. B **50**, 13 453 (1994).
[18] In order to emphasize the ability of neutron scattering to measure the vector property of the sample magnetization, we note that for instances where the magnetization reversed from one saturated state to the other via magnetization rotation, the sample magnetization never became zero.
[19] J. Nogués, D. Lederman, T. J. Moran, Ivan K. Schuller, and K. V. Rao, Appl. Phys. Lett. **68**, 3186 (1996).
[20] L. G. Parratt, Phys. Rev. **95**, 359 (1954).
[21] H. Dosch, Phys. Rev. B **35**, 2137 (1987).
[22] G. P. Felcher, R. O. Hilleke, R. K. Crawford, J. Hanmann, R. Kleb, and G. Ostrowski, Rev. Sci. Instrum. **58**, 609 (1987).
[23] C. F. Majkrzak, Physica (Amsterdam) **221B**, 342 (1996).
[24] Even an ensemble of domains with magnetizations equally likely to be $+90°$ or $-90°$ from the applied field will still produce SF scattering, if the scattering from each member of the ensemble adds incoherently; i.e., the size of the magnetic domain is larger than the coherent region (microns in size) of the neutron beam.
[25] Alternatively, rotation of the Fe magnetization out of the sample plane, such that no component of the sample magnetization lies in the sample plane, could also produce the conditions $\Delta\mathrm{NSF} \sim 0$ and $\mathrm{SF} \sim 0$; however, due to the thickness of the F layer, the demagnetization factor will tend to keep the magnetization in plane.
[26] B. H. Miller and E. D. Dahlberg, Appl. Phys. Lett. **69**, 3932 (1996).
[27] N. C. Koon, Phys. Rev. Lett. **78**, 4865 (1997).
[28] M. Kiwi, J. Mejia-Lopez, R. D. Portugal, and R. Ramirez, Appl. Phys. Lett. **75**, 3995 (1999).